



Not only does this design facilitate the production of phase-coherent RF and LO signals but it also allows initial phase-noise cancellation. The phase-noise operation can be seen in the block diagram, Fig. 1, where  $\Phi_v$  is the initial phase-noise. Most of the phase noise is cancelled in the down-conversion in the SIS-mixer and the remaining phase-noise, present at IF, is cancelled in the second down-conversion before the signal is fed into port two of the VNA for detection.

### III. MEASUREMENTS

As we mentioned earlier, the measurements have been performed with the sideband separation mixer, which will be used for Band 1 (221-275 GHz) of the facility receiver for Atacama Pathfinder Experiment (APEX). The use of a harmonic mixer, with an open ended waveguide, as the transmitting source results in a signal to noise ratio (S/N) close to 40 dB for an IF-bandwidth of 10 Hz. This shows the advantage of using the VNA as the signal source and detector, since this allows use of a very narrow detection bandwidth. Further decrease of detection bandwidth down to 1 Hz is feasible with a trade of the increased scan time. Measurement results from a scan approximately 55 mm away from the horn aperture are shown in Fig. 2 and Fig. 3. It should be pointed out that only a rough alignment has been done between the scanner and the cryostat for this measurement. The beam absolute position with respect to the receiver optics will be defined by the use of position sensitive detectors (PSD) and lasers but has not yet been implemented. It can be seen from the measured data, Fig. 2, that the beam appears to be nearly circular down to 30 dB.

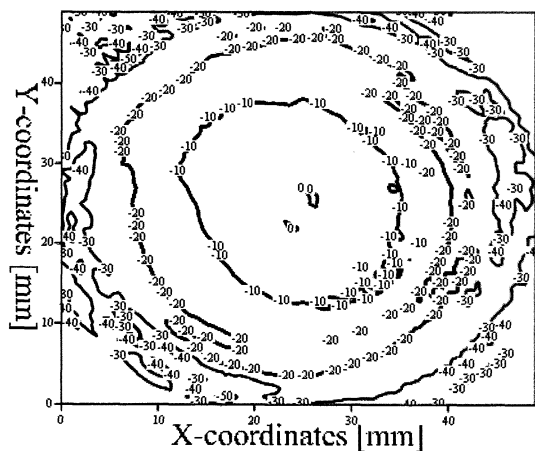


Fig. 2. Amplitude distribution of a scan performed at a cross-section at an approximate distance of 55 mm from the horn aperture.

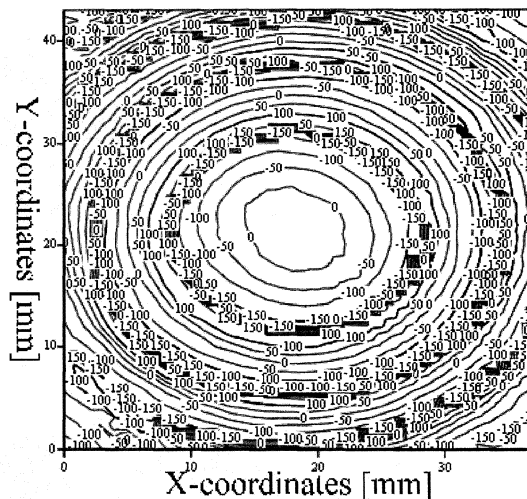


Fig. 3. Phase distribution of a scan performed at a cross-section at an approximate distance of 55 mm from the horn aperture.

To monitor the stability of the measurement, and add the possibility for calibration of the gain and the phase drifts in the system during the scan time, reference measurements were made. This was done by selecting a specific coordinate where the scanner returned to each time one row in the scan plane was completed. The reference plots can be seen in the Fig. 4 and the Fig. 5. The detected power varies less than 0.3 dB over the scan period, whereas the phase changes are less than 6 degrees, almost linear over the entire scan duration. To minimize the phase error due to cabling, all cables are fixed to preclude any movements except for a phase stable cable connecting the moving RF-source, placed on the scanner, to the fixed part of the system.

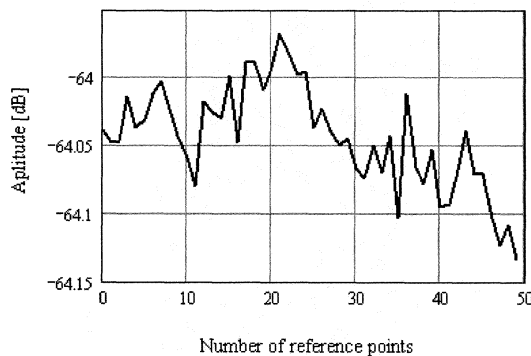


Fig. 4. Reference measurements of the amplitude taken at the same scan coordinate after the completion of each row. The amplitude varies less than 0.2 dB.

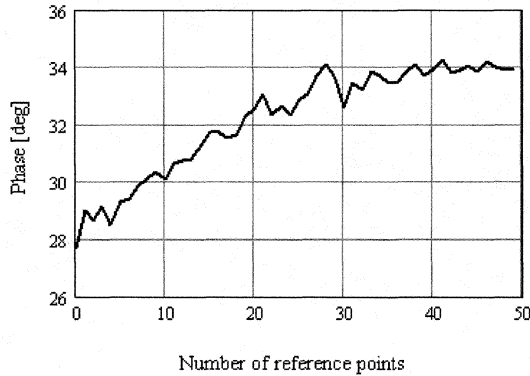


Fig. 5. Reference measurements of the phase taken at the same scan coordinate after the completion of each row. The phase increases, almost linearly, over the scan time.

To get an indication of possibilities to use a harmonic mixer as the RF-source even for higher frequency bands, the signal power was measured also at 341 GHz with the APEX Band 2 mixer [6] with a spectrum analyzer as detector. This measurement gave a S/N-ratio of 35 dB at a detection bandwidth of 1 kHz. The reason for using a spectrum analyzer instead of the VNA for detection was that the required filters for the set up with the VNA were not yet delivered. This, however, gives a promising indication that a harmonic mixer can be used as a signal source also for the higher bands, as the VNA set up is expected to offer even greater dynamic range with greatly reduced band.

#### IV. BEAM FITTING PROCEDURES

The measured amplitude and phase are combined into a complex beam, which is fitted to the fundamental Gaussian beam mode [7]

$$\psi_{00}(\Delta x, \Delta y) = \sqrt{\frac{2}{\pi\omega_x\omega_y}} \exp\left(-\frac{\Delta x^2}{\omega_x^2} - \frac{\Delta y^2}{\omega_y^2}\right) \times \exp(-j\beta_0(\frac{\Delta x^2}{2R_x} + \frac{\Delta y^2}{2R_y} + \delta_x \Delta x + \delta_y \Delta y)) \quad (1)$$

where  $\Delta x = x - x_c$  and  $\Delta y = y - y_c$ ,  $x$  and  $y$  are scan coordinates, whereas  $x_c$  and  $y_c$  are the scan coordinates for the amplitude center of the measured data [2].  $R_x$  and  $R_y$  are the radii of curvature of the phase front in  $x$ - and  $y$ -direction, respectively,  $\omega_x$  and  $\omega_y$  are the beam radii, and  $\delta_x$  and  $\delta_y$  are the tilt of the beam, in  $x$ - and  $y$ -direction, with respect to the normal of the scan plane. To derive the parameters ( $x_c$ ,  $y_c$ ,  $\omega_x$ ,  $\omega_y$ ,  $R_x$ ,  $R_y$ ,  $\delta_x$ ,  $\delta_y$ ) that best fit to the fundamental Gaussian beam mode, the measured data is fitted for the optimum power coupling coefficient [7]

$$K = \left| \sum_x \sum_y (E_{ComplexMeasured} \times \overline{E_{ComplexFitted}}) \right|^2 \quad (2)$$

where both the measured data and the fitted data are normalized to unity power over the area to be fitted. For the measured data in Fig. 2 and Fig. 3, a coupling coefficient to

the fundamental Gaussian mode of  $0.95 \pm 0.02$  was obtained when fitted down to -15 dB from the peak value. This coupling was slightly lower than expected, which we believe is the result of measurement errors due to standing waves and the beam truncation in the Dewar vacuum window. A higher coupling coefficient is expected once the standing waves are decreased. The fitting of the measured beam can be seen in Fig. 6 to Fig. 9, where the cross section, through the amplitude center, in  $x$ - and  $y$ -direction is presented.

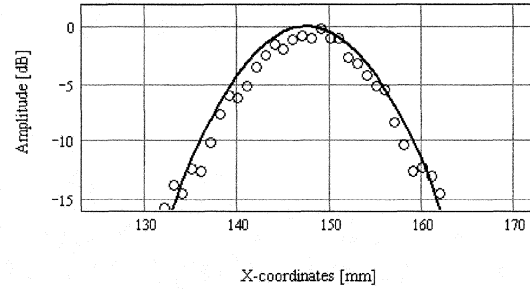


Fig. 6. Measured and fitted data for the amplitude (in dB) for the cross-section, in  $x$ -direction, at the amplitude center.

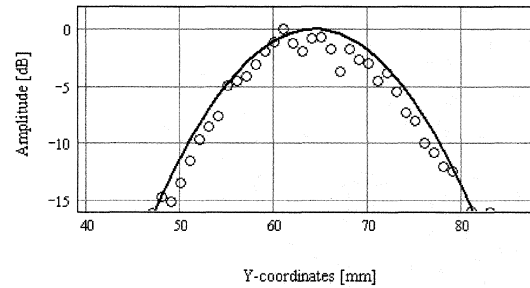


Fig. 7. Measured and fitted data for the amplitude (in dB) for the cross-section, in  $y$ -direction, at the amplitude center.

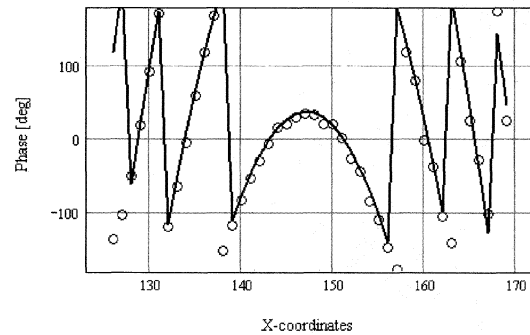


Fig. 8. Measured and fitted data for the phase (in degrees) for the cross-section, in  $x$ -direction, at the amplitude center.

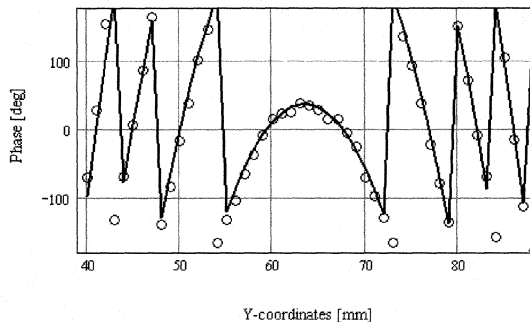


Fig. 9. Measured and fitted data for the phase (in degrees) for the cross-section, in y-direction, at the amplitude center.

Once the beam radius and the radius of curvature are fitted, the values can be used to calculate the size of the beam waist radius,  $\omega_0$ , and the distance from the amplitude center, located in the scan plane, to the waist location.

#### V. CONCLUSION

We have presented a vector measurement system for 221-275 GHz, which employs a combination of a single frequency source, a comb-generator, and a direct multiplication LO unit to achieve perfect phase-coherent RF- and LO signals as well as initial phase-noise cancellation. A dynamic range of about 40 dB has been demonstrated for measurements of the APEX Band 1 receiver. Since the presented set up is designed to cover also the higher bands (APEX-band 2 and 3) the RF-source has been tested at 341 GHz and the signal has been detected with a S/N-ratio of 35 dB with 1 kHz of the detection bandwidth. This is a very promising indication that we will be able to cover all three bands with our system by only switching two filters and the multiplication LO unit, since the use of a VNA as the phase detector allows us to decrease the detection bandwidth significantly and thereby attain even greater dynamic range.

#### ACKNOWLEDGMENT

The authors would like to thank Douglas Henke for all help during measurements, Magnus Svensson for his support with the Labview program, and Sven-Erik Ferm for his valuable help manufacturing hardware pieces. APEX Project is funded by the Swedish Research Council and the Wallenberg Foundation by their respective grants. Part of this work was supported by EU FP6 AMSTAR Program. We would like to thank Prof. H. Olofsson, Director, Onsala Space Observatory for his support.

#### References

- [1] M. T. Chen, C.E. Tong, R. Blundell, D.C. Papa, and S. Paine, "Receiver Beam Characterization for the SMA", in Proc. SPIE Conference on Advanced Tech. MMW, Radio, and THz Telescopes, Vol. 3357, pp. 106-113, Kona, Hawaii, Mars 1998.
- [2] C.-Y. E. Tong, D. V. Meledin, D. P. Marrone, S. N. Paine, H. Gibson, and R. Blundell, "Near Field Vector Beam Measurements at 1 THz",

IEEE Microwave and Wireless Components Letters, Vol. 13, No. 6, June 2003

- [3] C.-Y. E. Tong, D. n. Loudkov, S. N. Paine, D. P. Marrone, and R. Blundell, "Vector Measurements of the Beam Pattern of a 1.5 THz Superconducting HEB Receiver", 16<sup>th</sup> International Conference on Space Terahertz Technology-ISSTT 2005, Gothenburg, SWEDEN
- [4] W. Jellema, T. Finn, A. Baryshev, M. van der Vorst, S. Withington, J. A. Murphy, W. Wild, "Phase-Sensitive Near-Field Measurements and Electromagnetic Simulations of a Double-Slot HEB Integrated Lens-Antenna Mixer at 1.1, 1.2, and 1.6 THz", 16<sup>th</sup> International Conference on Space Terahertz Technology-ISSTT 2005, Gothenburg, SWEDEN
- [5] V. Vassilev, R. Monje, A. Pavolotsky, D. Dochev, D. Henke, and V. Belitsky, "A 211-275 GHz Sideband Separating SIS Mixer for APEX", 17<sup>th</sup> International Conference on Space Terahertz Technology-ISSTT 2006, Paris, France.
- [6] R. Monje, V. Belitsky, V. Vessen, A. Pavolotsky, I. Lapkin, "A 385-500 GHz SIS Mixer for APEX Telescope", presented at Astronomical Telescopes and Instrumentation, SPIE 2006, Orlando, Florida, USA
- [7] P. F. Goldsmith, "Quasi-optical Systems". New York: IEEE Press, 1998. ISBN 0-7803-3439-6.